JOURNAL OF MATERIALS SCIENCE 11 (1976) 1680–1690

Mechanical behaviour of the Cd-Zn eutectic composite

M. SAHOO, R. A. PORTER, R. W. SMITH
Department of Metallurgical Engineering, Queen's University, Kingston, Ontario, Canada

The structure and the resultant mechanical properties of the unidirectionally solidified Cd–Zn eutectic have been examined over a wide range of growth rates. The yield and ultimate strengths when tested in tension and compression were found to increase monotonically with the growth rate. The deformation of the matrix in tension occurred mostly by twinning whereas slip-controlled deformation was observed in compression. Hypereutectic alloys, directionally solidified at extremely fast growth rates to produce a coupled-eutectic microstructure, did not exhibit superior mechanical properties due to considerable misalignment of the reinforcing Zn phase.

1. Introduction

Following the division of binary eutectics into two broad groups [1], namely, regular (non-faceted/non-faceted) and anomalous (faceted/non-faceted), the present authors showed that further useful subdivisions into distinct structural types could be made by consideration of the entropy of solution (ΔS) and the volume fraction (V_f) of the minor phase [2–4]. Subsequently, the mechanical properties of that group of anomalous eutectics for which $V_f \simeq 6$ to 18% were examined [5–7] as part of a continuing broader examination of eutectic composites. In this work, it was of interest to examine the mechanical properties of some of the regular eutectics which have V_f values of similar proportion to that of the Al–Si eutectic. Of these, the Cd–Zn eutectic appeared particularly suitable since it has the appropriate volume fraction, 18% by volume of aligned Zn lamellae in a Cd matrix and information is available on the structure [8–10] and compressive properties [9] of this eutectic. In addition, both Cd and Zn have an hcp structure with a c/a ratio higher than the ideal and the eutectic was expected to behave as a single phase material so far as the mode of deformation is concerned. Shaw [9] examined the room temperature compressive behaviour of this eutectic directionally solidified at various rates and found that the yield strength increased with the freezing rate. However, the tensile behaviour of this eutectic has not been examined. Thus, one of the objectives of the present investigation was to more completely characterize the tensile and compressive properties of the Cd–Zn eutectic over a wide range of growth conditions. In addition, since an increasing growth rate produces finer microstructures and thereby enhances the possibility of achieving higher mechanical properties due to increased slip interference, the second aim of the investigation was to directionally solidify the eutectic at rates greater than reported previously and provide further information on the structure and mechanical properties.

Directional solidification of off-eutectic alloys has shown that aligned fully eutectic structures can be produced either at a high ratio of temperature gradient to a growth rate (G/R) [11–13], or by employing high growth rates [14, 15]. In this way the volume fraction of the reinforcing phase can be varied simply by growing off-eutectic compositions at favourable growth conditions. Thus additional experiments were carried out to determine the mechanical properties of certain hypo- and hypereutectic Cd–Zn alloys.

2. Experimental

99.999% purity components were weighed to the eutectic composition given by Hansen [16], sealed in argon-filled Pyrex tubes, heated in a gas flame to melt the constituents and shaken vigor-

ously to ensure homogenization. The solidified rods were swaged to 5 mm diameter to promote macro-homogeneity. The rods were sealed into argon-filled 6 mm i.d. Pyrex tubes and directionally solidified by lowering the alloy through a tube-furnace set at 550° C into a water jacket located 1.5 cm below the furnace. It was found from preliminary measurements with thermocouples sealed into the specimen tube, that the growth velocity was equal to the lowering rate over most of the specimen length for the range of growth velocities used. The temperature gradient in the liquid at the solid-liquid interface was approximately $6^{\circ}\,C\,mm^{-1}$ for a growth rate of $155\,mm\,h^{-1}$, being similar to that used by Shaw [9]. Off-eutectic compositions in the range 16 to 23 wt % Zn were prepared and directionally solidified in a similar manner.

The first and last 3 cm of each alloy were rejected and the tensile and compressive testing specimens were cut from the remainder. Longitudinal and transverse sections were prepared for metallographic examination.

Specimens for tensile testing were machined in a jeweller's lathe to produce a reduced diameter of 3.8 mm. Compressive specimens, 12.0 mm long and 5.0 mm diameter, were carefully polished to produce parallel faces and then etched to remove any worked layer. All tensile and compressive tests were performed at ambient temperatures (~ 25° C) with the stress axis parallel to the growth axis, using an Instron testing machine at a cross head speed of $\sim 0.13\,mm\,min^{-1}$. In the case of tensile tests, a 25.4 mm Instron extensometer was used to measure specimen elongations.*

Metallographic specimens were cold mounted, polished in the conventional manner and finally etched in a solution of 320 g CrO_3, 20 g Na_2SO_4, and 1000 ml H_2O.

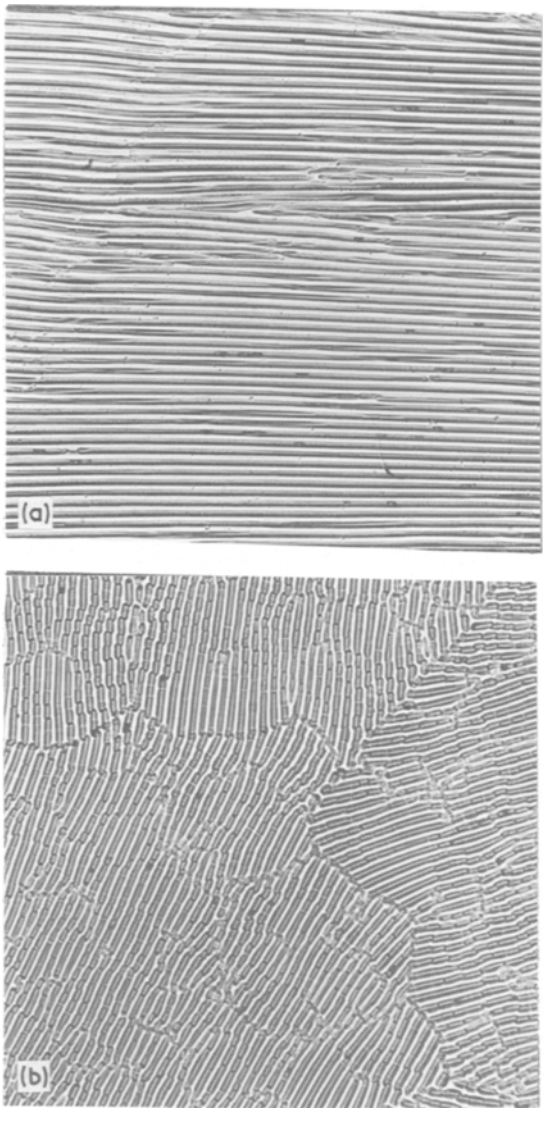

Figure 1 Optical micrographs of the directionally solidified Cd–Zn eutectic showing the lamellar structure. Growth rate = $2.9\,mm\,h^{-1}$ (× 400): (a) longitudinal section; (b) transverse section.

3. Results and discussion

3.1. Microstructure

Metallographic examination revealed that the solidification rate greatly influenced the eutectic morphology. A well developed lamellar microstructure was produced up to a growth rate of $400\,mm\,h^{-1}$ (Fig. 1a and b). Fig. 1b shows traces of mismatch interfaces and grain boundaries. It is evident from Fig. 1a that the Zn phase is oriented parallel to the direction of growth. The growth direction of the lamellar eutectic has been previously established as the close-packed $\langle 1\,1\,\bar{2}0\rangle$ direction [9, 17]. At growth rates greater than $400\,mm\,h^{-1}$ a cellular eutectic structure appeared

*In order to determine the effect of machining on the tensile properties of the Cd–Zn eutectics, some of the machined tensile samples were packed in alumina in pyrex tubes, unidirectionally solidified and pulled in tension as before. No systematic and significant differences were observed between the tensile properties of the machines and those of the regrown specimens.

(Fig. 2a and b). The cellular microstructure is a consequence of constitutional undercooling which is induced by high growth rates, low temperature gradients at the solid–liquid interface and/or increasing impurity concentrations.

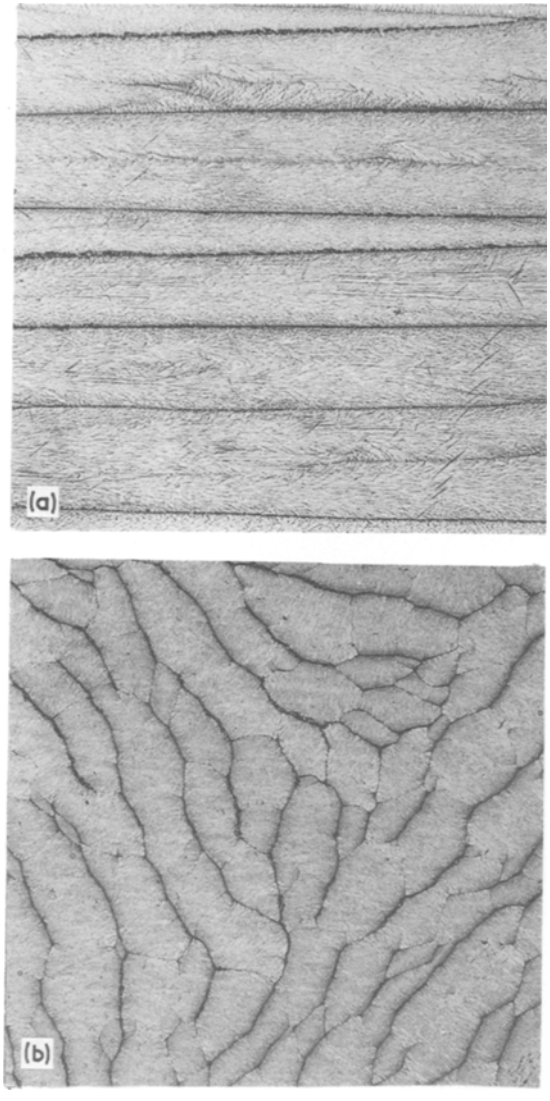

Figure 2 Optical micrographs of the directionally solidified Cd–Zn eutectic showing the cellular structure. Growth rate = 1600 mm h^{-1} (× 100): (a) longtiudinal section; (b) transverse section.

At the solid–liquid interface, the temperature gradients in the solid and liquid, G_s and G_L, are related by

$$K_s G_s = K_L G_L + LR \qquad (1)$$

where K_s and K_L are the thermal conductivities in the solid and liquid respectively, L is the latent heat of fusion and R is the growth velocity. Since the distance between the tube furnace and the water jacket was fixed for all growth rates, with increasing growth rates the interface moves closer to the water jacket. Hence, G_L decreases with increasing growth rates to permit constitutional supercooling to arise. At extremely fast growth rates the interface can move into the water jacket and hence the interface can become concave to the liquid and so promote further misalignment of the lamellae inside each cell. It was observed that when the colony structure was produced, the Zn phase was oriented parallel to the growth direction only in the centre of the cells. However, away from the cell centres considerable fanning of the Zn phase towards cell walls has been observed. The cell boundaries exhibited a much coarser structure than the central parts. The cell size was found to decrease with increasing growth rates, obeying a relationship of the type:

$$d_c \propto R^{-2/3}. \qquad (2)$$

According to Tiller and Mrdjenovich [8], the breakdown of the lamellar morphology to a colony structure should occur at a growth rate about 2200 mm h^{-1}, whereas in the present studies a cellular microstructure was observed even at 1200 mm h^{-1}. This discrepancy may be attributable to some impurity effect since Tiller and Mrdjenovich used "zone" refined metals of exceptionally high purity, so that constitutional undercooling sets in here at a relatively lower growth rate.

To directionally solidify the off-eutectic compositions it was necessary to investigate the range of "coupled" euctectic growth in the Cd–Zn system. To do this the high growth rate technique [14, 15] was employed. Fig. 3 illustrates the range of compositions as a function of growth rate where a coupled-eutectic microstructure can be obtained. This figure shows that in common with the Al–Ni and Al–Co systems [15] the zone of the "coupled" growth is skewed towards the hypereutectic compositions. Because of the employment of fast growth rates to prevent the formation of either Zn or Cd primaries, constitutional undercooling could not be avoided and a fine cellular structure was produced in all cases.

The interlamellar spacing, λ, measured on the transverse sections of the unidirectionally solidi-

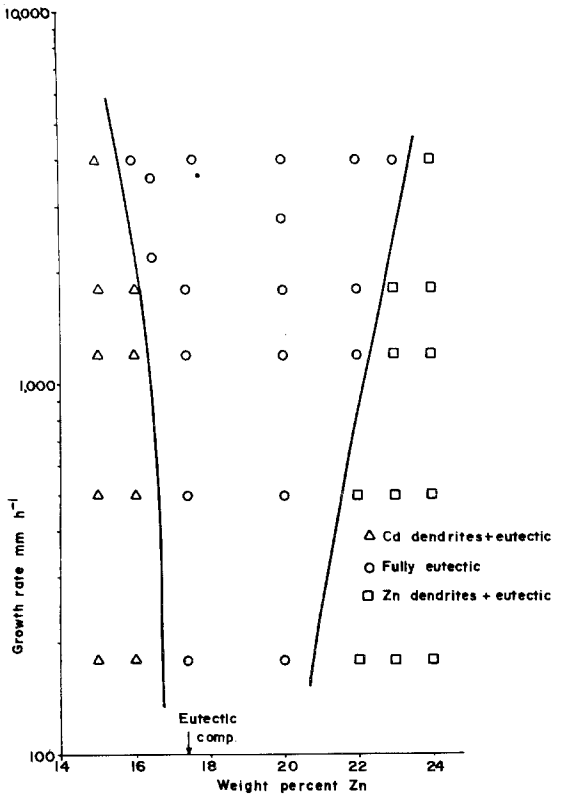

Figure 3 Composition–growth rate plot showing the range of coupled-eutectic microstructure.

fied Cd–Zn eutectic has been previously found [8, 9] to fit a relationship of the type:

$$\lambda = AR^{-1/2} \quad (3)$$

In the present work, similar values for λ were found as a function of R to those described in [8] and [9]. Interlamellar spacing of the cellular specimens grown at extremely fast rates were not determined because of the misalignment.

3.2. Mechanical properties

3.2.1. Elastic modulus

The average modulus of all specimens calculated from the slope of the tensile stress–strain curves was found to be about 79×10^3 N mm^{-2} or 11.5×10^6 psi, and no regular variation of the modulus with freezing rate was observed. This is greater than that measured by Shaw [9] who, using ultrasonic techniques, obtained an average Young's modulus of 54×10^3 N mm^{-2} or 7.9×10^6 psi, in the $\langle 1\,1\,\bar{2}\,0\rangle$ direction.

Assuming that there is no interaction between the two phases, the elastic modulus of the composite might be expected to obey the rule of mixtures; i.e. be the volume fraction weighted mean of the individual moduli of the two phases as expressed in Equation 4, namely,

$$E_c = E_f V_f + E_m V_m \quad (4)$$

where E is the elastic modulus, V is the volume fraction and subscripts c, f and m refer to composite, fibre and matrix respectively. Using the elastic compliances [18], the elastic modulus of Zn lamellae (E_f) and Cd matrix (E_m) in the $\langle 1\,1\,\bar{2}\,0\rangle$ direction are respectively 119×10^3 N mm^{-2} or 17.2×10^6 psi, and 78×10^3 N mm^{-2} or 11.3×10^6 psi. Substitution of the experimentally determined value for E_c (79×10^3 N mm^{-2}) and the calculated value for E_m (78×10^3 N mm^{-2}) into Equation 4 predicts a value for E_f of 83×10^3 N mm^{-2} or 12×10^6 psi, for the Zn lamellae in the $\langle 1\,1\,\bar{2}\,0\rangle$ direction. This is smaller than the theoretically calculated value by a factor of 0.7. The experimentally measured smaller E_c values tend to indicate that the reinforcing phase is perhaps imperfect and contains many dislocations Similar conclusions were derived by Coleman *et al.* [19] who found that for Zn whiskers, with diameters in the range of 1 to 10 μm and with their axes in a $(1\,0\,\bar{1}\,0)$ plane, the experimentally measured moduli turned out to be consistently smaller than the accepted value by a factor of roughly 0.7.

3.2.2 Deformation behaviour

The results of the tension and compression tests are summarized in Table I. Typical room temperature tensile stress–strain curves are shown in Fig. 4a. These curves are drawn only up to the UTS of the eutectic. In each of the tensile tests failure did not occur at the UTS. Instead, the load dropped gradually as considerable necking appeared in the gauge length such that, when fracture took place, the plastic strain exceeded 7%. This is why Table I shows only the uniform elongation measured by the strain gauge. These features tend to indicate that the reinforcing Zn phase becomes plastic after the UTS. Thus the directionally solidified Cd–Zn eutectic can be classified as a ductile composite since it exhibits large elongations before rupture as opposed to brittle composites where fibre fracture leads to immediate failure of the composite with a total fracture strain of 1 or 2%.

The deformation behaviour of other ductile composites has been discussed by Bibring [20]. In

TABLE I Room temperature mechanical properties of directionally solidified Cd–Zn eutectics

Growth rate ($mm\ h^{-1}$)	Tension			Compression		
	0.2% Off-set yield strength ($N\ mm^{-2}$)	UTS ($N\ mm^{-2}$)	Uniform elongation (%)	0.2% Off-set yield strength ($N\ mm^{-2}$)	UCS ($N\ mm^{-2}$)	Uniform elongation (%)
As-cast	34.0	57.0	8.0	79	120	5.3
2.9	101.0	107.0	4.7	169	173	0.3
				175	178	0.3
12.0	91.0	97.4	4.0	171	171	0.2
	98.0	110.0	3.5	177	178	0.2
	87.0	92.0	3.0			
	103.0	111.0	3.0			
36.0	110.0	121.5	4.0	197	207	0.5
				189	196	0.4
120.0	111.0	127.0	5.0	210	236	1.0
	110.0	125.0	4.5	207	224	0.8
	107.0	124.0	4.8			
155.0	112.0	136.0	5.5	224	240	0.5
	123.0	139.0	4.7	231	241	0.4
400.0	126.5	141.0	4.2	276	295	0.6
1200.0	133.0	141.0	1.0			
	123.0	134.0	2.8	337	365	0.5
	125.0	138.0	3.0	341	360	0.3
1600.0	128.0	140.0	3.0	331	360	0.5
				331	344	0.4
2800.0	155.0	162.0	0.8	378	397	0.3
				368	397	0.4
4000.0	156.0	165.0	1.0	357	420	0.7
	168.0	186.0	1.5			

the case of the Ni–Ni_3Nb eutectic [21], the large strains have been associated with the twinning of the reinforcing phase. In the systems examined here, both Cd and Zn have an hcp structure and should twin easily in $(1\,0\,\bar{1}\,2)$ planes either in tension or in compression depending on orientation [22, 23]. Deformation twins were, in fact produced in the Cd–Zn eutectic when tested in tension. This was revealed by metallographic examination of the fractured specimens; e.g. Fig. 5a and b, for the lamellar and cellular microstructure. Also the tensile stress–strain curves showed discontinuous strain increments due to twinning and audible clicks could be heard during each load drop due to twin nucleation. This gave the recorded stress–strain curve a saw-tooth appearance, see Fig. 4b. However, for the sake of clarity, such jagged irregularities in the stress–strain curves are not shown in Fig. 4.

In general, the load drops started after about 0.15% composite strain. It was also noticed that for the lamellar microstructures the load drops continued up to about 3% composite strain, whereas for the cellular microstructures, load drops were observed only near the yield region. Each twin band was lenticular in shape and was insensitive to repeated polishing/etching.

In the Cd–Zn eutectic the c/a ratio for Cd and Zn are 1.886 and 1.856 respectively. In both phases the growth direction is parellel to $\langle 1\,1\,\bar{2}\,0\rangle$. The relative orientations of the two phases have been established [17, 24] as $(0\,0\,0\,1)_{Cd} \| (0\,0\,0\,1)_{Zn}$ and $[0\,1\,\bar{1}\,0]_{Cd} \| [0\,1\,\bar{1}\,0]_{Zn}$. There is complete epitaxy between the alternate Cd and Zn layers so the composite might be expected to behave as a single phase material, the twins extending across individual eutectic grains. This is clearly evident in Fig. 5 and has also been reported by Vogel [25]. Confirmation of this behaviour is seen in the fact that many pairs of twins intersected at approximately 90° corresponding closely to the 86° angle separating equivalent $\{1\,0\,\bar{1}\,2\}$ twinning planes. It is

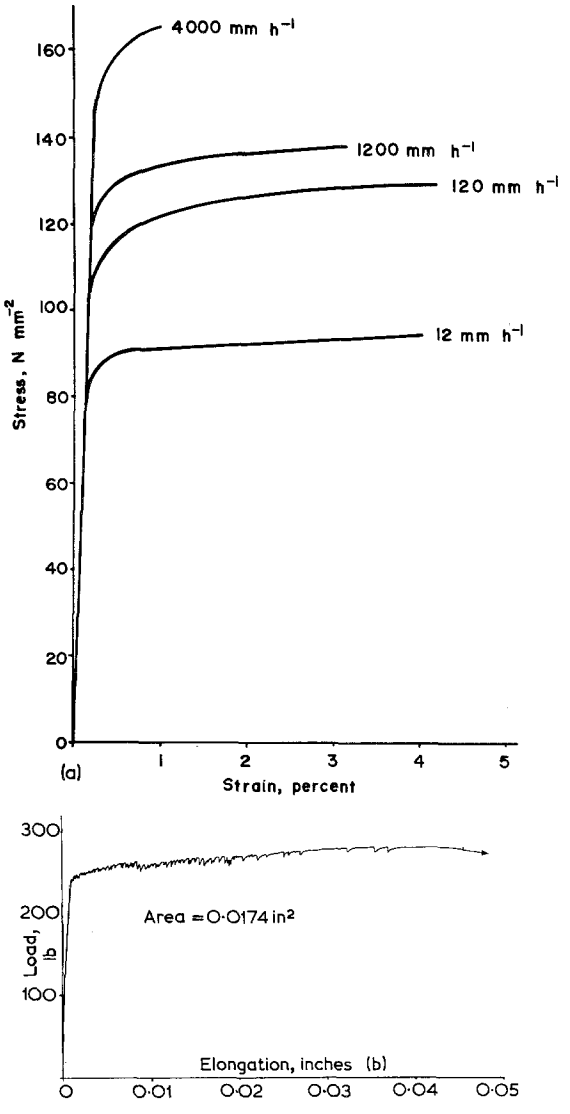

Figure 4 (a) Room temperature engineering tensile stress–strain curves for Cd–Zn eutectic alloys directionally solidified at various rates. (b) Typical tensile load–elongation curve for the directionally solidified Cd–Zn eutectic showing the saw-tooth appearance. Growth rate $= 12\,\text{mm}\,\text{h}^{-1}$.

further noted that the twins paired easily across cell walls thus showing that the misorientations between individual colonies within a single eutectic grain are very small.

It is well known that twinning will occur for a particular sense of applied stress [22, 23] depending on the crystal orientation and the twin mode. Thus for the Cd–Zn eutectic with tensile stress axis parallel to $\langle 1\,1\,2\,0\rangle$, $\{1\,0\,\bar{1}\,2\}$ twinning is caused by tensile stress and not by compressive stress. Metallographic examination of the compressed samples did not reveal any twin bands. Instead slip lines (smoothly bent lamellae) kinks (sharply bent lamellae) and cross-slip patterns, Fig. 6a which have previously described for Cd–Zn [9, 10] and Al–$CuAl_2$ [26] eutectics tested in compression, were observed. These features tend to indicate that deformation in compression is controlled by slip alone*. Since the lamellar interfaces are common $\{0\,0\,0\,1\}$ planes with the growth direction $\langle 1\,\bar{1}\,\bar{2}\,0\rangle$

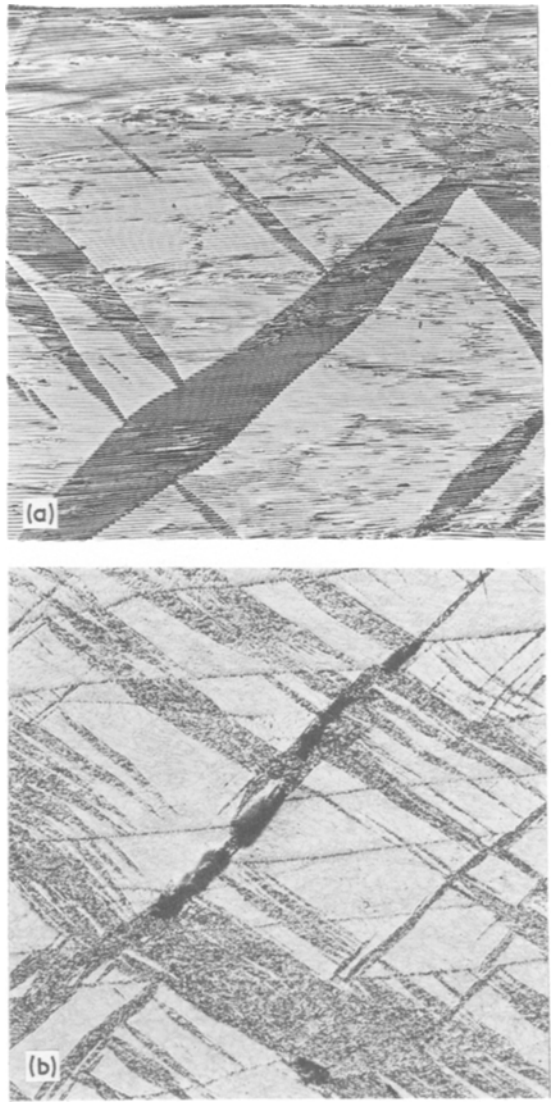

Figure 5 Optical micrographs of longitudinal sections near the fracture surface of the Cd–Zn eutectic alloys showing the deformation twins. (a) Growth rate $= 120\,\text{mm}\,\text{h}^{-1}$, fracture strain = 9% (× 200). (b) Growth rate $= 4000\,\text{mm}\,\text{h}^{-1}$, fracture strain = 5% (× 300).

*Hall notes that the $<11\bar{2}0>$ compression axis does not permit twinning in zinc.

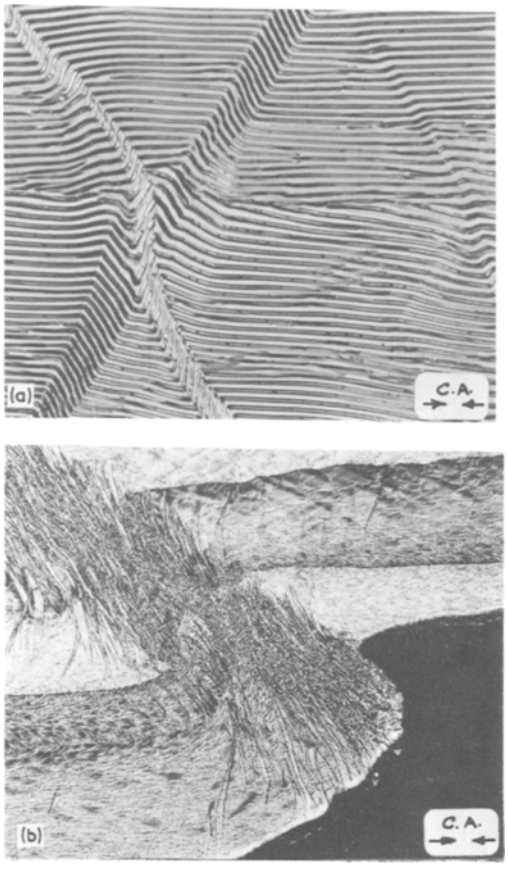

Figure 6 Optical micrographs of the compressed Cd–Zn eutectic alloys. (C.A. = compression axis): (a) showing kinks, slip lines and cross-slip patterns, growth rate = 12 m h^{-1}, 2.5% strain (×470); (b) showing massive steps on the surface, growth rate = 2800 mm h^{-1} (×150).

and the $\{1\,\bar{1}\,0\,0\}$ prism planes at right angles to the compression axis, the planes on which slip is occurring must be $\{1\,1\,\bar{2}\,2\}$ pyramidal planes [27 28]. Such slip causes massive steps in the surface of the specimens with a cellular microstructures (Fig. 6b), and general barrelling of the specimens solely with lamellar microstructures.

3.2.3. Effect of solidification rate

The effect of solidification rate on the tensile and compressive strength data is illustrated in Fig. 7. It is evident from Table I and Fig. 7 that directionally solidifying the Cd–Zn eutectic at very low growth rates almost doubled the tensile and compressive strength properties relative to those of the as-cast eutectic. Further increases in growth rates caused a decrease in eutectic spacings and a corresponding increase in both the tensile and compressive strength values, the increases in the latter case being more significant.

The reasons for these increases in strength are not clear. It might be expected that an increase should accompany structural refinement in any system since the increased interphase boundary frequency provides more opportunities for dislocation pile-ups. However, in the lamellar eutectic, the cadmium and zinc-rich phases grow with a common $\{0\,0\,0\,1\}$ habit and in the same $\langle 0\,1\,\bar{1}\,0\rangle$. This expitaxial arrangement would be complete except for the fact that the a-spacing of each phase differs by 10%. Thus the semicoherent interphase boundary must contain a regular but widely spread dislocation array. Such an array is unlikely to provide much dislocation pile-up and so contribute significantly to the increase in strength accompanying structural refinement, as proposed by Shaw [9]. A much more likely source of dislocation movement hindrance is that arising from the increasingly large number of grown-in crystal defects accompanying higher freezing rates. Such defects would hinder both glissile and twinning dislocations. Some support for this arrangement is to be found in Fig. 5 where twins are seen to cross lamellar boundaries but increase in frequency as the growth rate is increased. One complication in attempting any simple explanation of the increase in both tensile and compressive strength with growth rate is that fast freezing produces a cellular interface. As a result of the cell curvature, the lamellae "fan-out" towards the cell walls. The maintenance of the same habit and epitaxy as in regular lamellar form would require that even further growth defects arise since the interlamellar boundary is always normal to the solid–liquid interface. These local variations in orientations would promote increased dislocation interference and consequent increases in observed strengths.

It is noted that the present compression data compares well with those of Shaw's [9]. However, Shaw observed that the directionally solidified lamellar eutectics, when tested in compression, all showed a sharp yield point, with little or no pre-yield microstrain, followed by a considerable drop in load. A few of the load elongation curves also gave what appeared to be a lower yield point followed by work hardening. This yield point phenomenon was not observed in the present investigation.

Shaw [9] plotted the compressive yield stress of the Cd–Zn eutectic in terms of the Hall–Petch $\lambda^{1/2}$ relationship and attempted a rationalization in

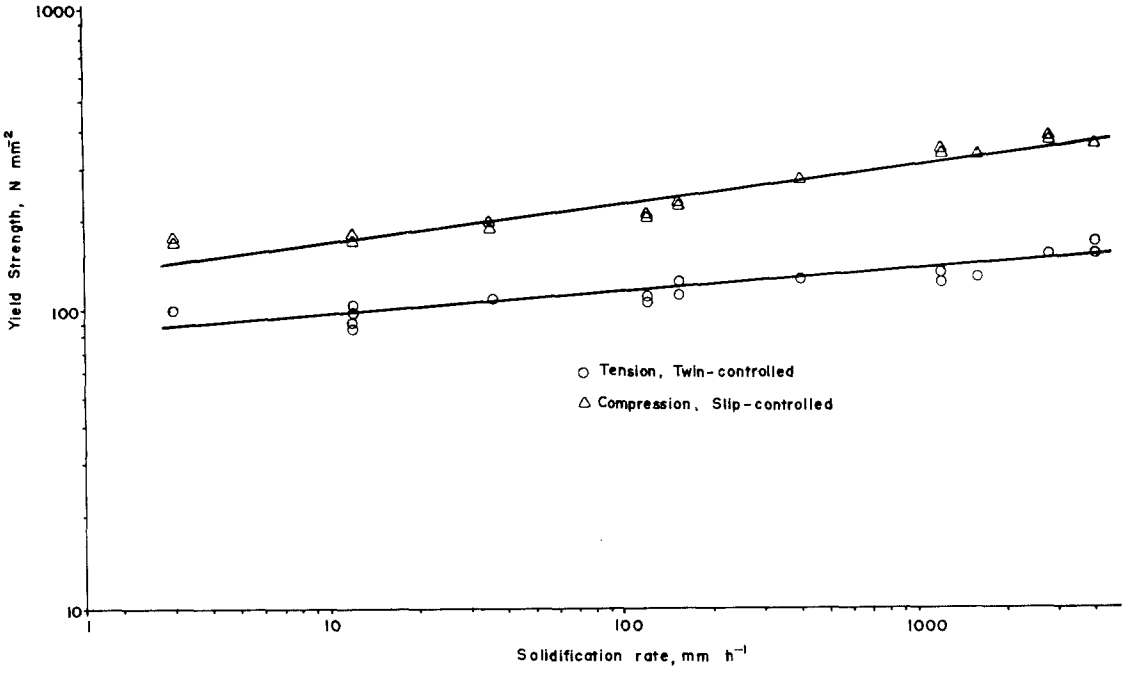

Figure 7 Effect of solidification rate on the tensile and compressive yield strength (0.2% off-set).

terms of a dislocation pile-up model. However, Chadwick [29] has recently reviewed the relationship between the microstructural spacings and the mechanical properties of the eutectic composites and has pointed out that $\lambda^{-1/2}$ Hall–Petch plots are plotted more on the grounds of familiarity than on facts and that the published figures can be recorded, often equally well as λ^{-1} plots and in some cases as straight λ plots. To avoid this criticism, since λ is related to the solidification rate, the composite yield stress may be expressed as [30]:

$$\sigma = \sigma_0 + \sigma(R) \tag{5}$$

where σ_0 is independent of solidification rate and obtainable from the intercept of the logarithmic plot of σ versus R. The second term $\sigma(R)$ can again be expressed as

$$\sigma(R) = kR^n \tag{6}$$

where k is a constant. k and n can be obtained from the intercept and slope of the logarithmic plot of $\sigma(R)$ versus R. Following this, in the present work, the two equations relating the solidification rate with the slip-controlled and twin-controlled yield stress may be expressed as, respectively,

$$\sigma = 92 + 22R^{0.25} \tag{7}$$

$$\sigma = 70 + 12R^{0.20} \tag{8}$$

Taking note of the possible errors in these expressions, we consider that both processes may be adequately described in the equation

$$\sigma = \sigma_0 + KR^{0.25} \tag{9}$$

Recalling that the interlamellar spacing of the eutectic is proportional to the inverse square root of the growth rate, the yield stress dependence on the inverse fourth root of the solidification rate tends to indicate that the yield stress should be proportional to the inverse square root of the interlamellar spacing. Whilst this appears to fit the Cd–Zn eutectic, separate power laws were required to describe the two deformation processes in Mg–Mg_2Ni eutectic [30], a system in which the reinforcing Mg_2Ni phase does not deform.

It may be noted from Table I that for each growth condition the compressive yield and ultimate strengths are higher than the respective tensile properties. A similar difference to that observed in this work has been reported for other eutectics [5–7, 31–33]. This form of response has been previously interpreted in terms of residual stresses due to differences in the coefficients of thermal expansion of the two phases in each eutectic. In the earlier reported cases the thermal expansion coefficient of the matrix was greater than that of the reinforcing phase. Thus, following

directional solidification, the former will be in a state of tension and is therefore expected to yield at a lower stress level in tension than in compression. In the case of the Cd–Zn eutectic, the thermal expansion coefficients for Cd and Zn perpendicular to the hexad axis are 42×10^{-6} and 12.3×10^{-6} K^{-1} respectively [34–36]. The superior compressive strengths may be then accounted for by the presence of the thermally induced residual stresses produced during cooling from the eutectic temperature to the room temperature. However, the nature of the operating deformation modes should also be taken into account to explain the superior compressive strengths. In tension the Cd-Zn eutectic deforms by twinning after the onset of plasticity in the composite. By contrast deformation in compression takes place only by slip and the Zn lamellae are required to buckle. Twins can nucleate in Zn and Cd at lower stress levels, whereas higher stresses will be required to achieve the non-basal slip necessary for buckling. Thus, the tensile strengths should be lower than the compressive strengths. Similar behaviour has been observed for the Mg–Mg_2Ni eutectic [30] where for a particular crystallographic orientation the lower tensile yield strength of the composite was attributed to the yielding of the Mg matrix in tension by twinning while compressive yielding by non-basal slip resulted in superior compressive properties. A somewhat different argument has been advanced by Hoover and Hertzberg [21] for the observed mechanical properties of the ductile Ni–Ni_3Nb eutectic composite. They observed that the final composite rupture in the Ni–Ni_3Nb eutectic was achieved by Ni_3Nb failure along twin boundaries and subsequent necking of the intervening Ni lamellae and so concluded that the superior compressive strength of this composite may be accounted for by the absence of compressive deformation mechanisms leading to the cracking at twin boundaries observed in tension. The twin–matrix interface is a region of considerable strain and so it may be possible for fracture to occur there in preference to any other crystallographic plane in the allow. Twin boundary cracking was observed also in the present case (Fig. 5b). Optical microscopic examination of longitudinal sections through the fracture surface of the lamellar eutectics showed broken Zn lamellae close to the fracture surface (Fig. 8a). In cellular specimens the caviation leading to failure

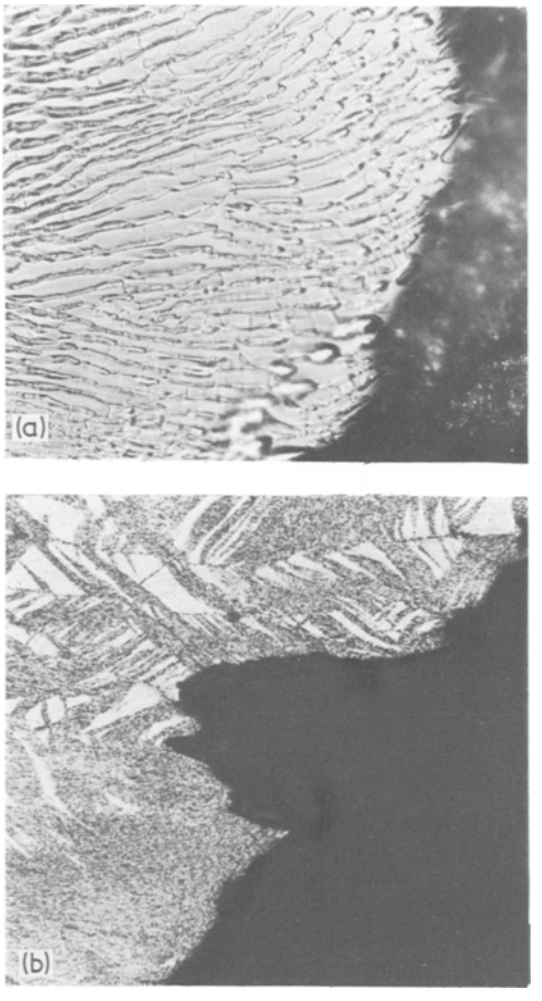

Figure 8 Optical micrograph of the tensile fracture surface of the Cd–Zn eutectic alloys. (a) Growth rate = 2.9 mm h^{-1} (× 470). (b) Growth rate = 4000 mm h^{-1} (× 220).

appear to originate at cell walls (Fig. 8b). It is noted that these are regions in which the second phase is coarse and often missing. Because of this they would expected to be mechanically weaker and so fail at a somewhat lower stress than other regions.

3.2.4. Off-eutectic composition

The tensile and compressive strength data for the off-eutectic compositions are presented in Table II. It is evident that although the volume fraction of the reinforcing phase has been varied from 0.16 to 0.25, the tensile and compressive strength values remain unchanged in relation to the strength of the eutectic alloys at similar growth conditions. The eutectic and off-eutectic alloys

TABLE II Room temperature mechanical properties of directionally solidified off-eutectic Cd–Zn alloys

Wt % Zinc	V_f	Growth rate (mm h^{-1})	Micro-structure*	Tension			Compression		
				0.2% off-set yield strength (N mm^{-2})	UTS (N mm^{-2})	Uniform elongation (%)	0.2% off-set yield strength (N mm^{-2})	UCS (N mm^{-2})	Uniform elongation (%)
16.0	0.16	4000.0	C	151	165	1.7	340	400	0.7
							342	404	0.7
			C+D	150	167	1.7	181	209	2.0
							171	207	2.5
16.5	0.17	2100.0	C	157	170	1.3	364	392	0.4
		3600.0	C	152	165	1.7	346	415	0.7
							365	411	0.6
20.0	0.21	2800.0	C	146	152	0.7	370	378	0.3
				153	164	1.4	378	383	0.3
22.0	0.23	4000.0	C	155	164	1.1	368	396	0.5
				170	177	0.7	354	402	0.6
23.0	0.24	4000.0	C	165	170	0.6	354	387	0.7
							344	386	0.7
			C+D	168	173	1.2	138	165	3.0
							187	204	1.5

*C, cellular, D, dendritic.

exhibit a cellular microstructure at such growth rates. If the matrix work-hardening effects due to the presence of the reinforcing Zn phase is assumed to be the same in all the alloys for a given interlamellar spacing, the presumed beneficial effects of a higher volume fraction of the reinforcing phase are not evident in the hypereutectic alloys. Thus it may be concluded that either the reinforcing Zn phase is imperfect and contains many surface defects due to imposed growth restrictions or that its fracture strength is not as high as may be estimated from lamellar eutectic alloys. Alternatively, if regular lamellae of the reinforcing phase contribute most to the strength of the composite [37], cellular specimens would be expected to be weaker in general than the truly lamellar counterparts because many side lamellae are curved away from the principal axis.

Some of the off-eutectic alloys were deliberately directionally solidified at lower temperature gradients to produce Cd and Zn primaries in the hypo- and hypereutectic alloys respectively. It is seen from Table II that the presence of these primaries did not alter the tensile properties. However, deterioration of compressive strength and improvement of ductility result.

4. Conclusions

(1) The Cd–Zn eutectic has been directionally solidified at rates of 2.9 to 4000 mm h^{-1}. Its lamellar microstructure was replaced by a cellular structure at growth rates greater than 400 mm h^{-1}. The interlamellar spacings and cell size decreased with increasing growth rates.

(2) Room temperature tensile and compressive strengths were found to increase with increasing growth rates. No dramatic increases in mechanical properties at high growth rates were observed, presumably because of the misalignment of the reinforcing Zn phase within the cell walls produced by directional solidification at such rates.

(3) The eutectic exhibited large ductility at each growth rate and so may be described as a ductile matrix–ductile lamellae composite.

(4) The deformation mode of the composite was found to be controlled by twinning in tension and by slip in compression.

(5) The hypereutectic alloys, directionally solidified at fast growth rates to produce a coupled-eutectic misrostructure, did not show the promise of attaining high tensile and compressive strengths probably because of the misaligned Zn phase.

Acknowledgements

The authors wish to thank Dr W.B.F. Mackay for his interest and for the provision of laboratory facilities The financial support of the National Research Council of Canada is also greatefully acknowledged.

References

1. J. D. HUNT and K. A. JACKSON, *Trans. Met. Soc. AIME* **242** (1966) 843.
2. M. N. CROKER, R. S. FIDLER and R. W. SMITH, *Proc. Roy. Soc.* **A335** (1973) 15.
3. M. N. CROKER, M. McPARLAN, D. BARAGER and R. W. SMITH, *J. Crystal Growth* **29** (1975) 85.
4. M. N. CROKER, D. BARAGER and R. W. SMITH, *ibid* **30** (1975) 198.
5. M. SAHOO and R. W. SMITH, *Met. Sci.* **9** (1975) 217.
6. *Idem, Canad. Met. Q.* **15** (1976) 1.
7. *Idem, J. Mater. Sci.* **11** (1976) 1125.
8. W. A. TILLER and R. MRDJENOVICH, *J. Appl. Phys.* **34** (1963) 3639.
9. B. J. SHAW, *Acta Met.* **15** (1967) 1169.
10. B. SOUTIERE and H. W. KERR, *Trans. Met. Soc. AIME* **245** (1969) 2595.
11. F. R. MOLLARD and M. C. FLEMINGS, *ibid* **239** (1967) 1534.
12. K. A. JACKSON, *ibid* **242** (1968) 1275
13. R. M. JORDAN and J. D. HUNT, *Met. Trans.* **2** (1971) 3401.
14. H. E. CLINE and J. D. LIVINGSTON, *Trans. Met. Soc. AIME,* **245** (1969) 1987.
15. R. S. BARCLEY H. W. KERR and P. NIESSON, *J. Mater. Sci.* **6** (1971) 1168.
16. M. HANSEN, "Constitution of Binary Allows" (McGraw-Hill New York, 1958).
17. W. STRAUMANIS and N. BRAKSS, *Z. Phys. Chem.* **30B** (1935) 117.
18. H. B. HUNTINGTON, *Solid State Phys.* 7 (1958), 278.
19. R. V. COLEMAN B. PRICE and N. CABRERA, *J. Appl. Phys.* 28 (1957), 1360.
20. H. BIBRING, Proceedings of the Conference on In-Situ Composites, Vol. II, National Academy of Sciences – National Academy of Eng. (1973) p.1.
21. W. R. HOOVER and R. W. HERTZBERG, *Met. Trans.* 2 (1971) 1283.
22. E. SCHMID and W. BOAS, "Plasticity of Crystals" (Hughes London, 1950) p. 96.
23. E. O. HALL, "Twinning" (Buttersworth, London, 1954) 42.
24. D. D. DOUBLE and A. HELLAWELL, *J. Crystal Growth* **6** (1969) 107.
25. R. VOGEL, *Anorg. Chem.* **154** (1926) 399.
26. A. S. Yue, F. W. CROSSMAN, A. E. VODOZ and M. I. JACOBSON, *Trans. Met. Soc. AIME* **242** (1968) 2441.
28. J. H. WENICK and E. E. THOMAS, *ibid* **218** (1960) 763
29. G. A. CHADWICK, Met. Sci. 9 (1975) 300
30. K. H. ECKELMEYER and R. W. HERTZBERG, *Met. Trans.* 3 (1972) 609.
31. E. R. THOMPSON, D. A. KOSS and J. C. CHESTNUT, *ibid* **1** (1970) 2807.
32. A. PATTANAIK and A. LAWLEY, *ibid* **2** (1971) 1529.
33. W. R. KRUMMHEUER and H. ALEXANDER, *J. Mater. Sci.* 9 (1974) 229.
34 J. MEDOFF and I. CARDOFF, *Trans. Met. Soc. AIME* **230** (1964) 246.
35. N. MADAIAH and G. M. GRAHAM, *Canad. J. Phys.* **42** (1964) 221.
36. D. A. CHANNING and S. WEINTROUB, *ibid* **43** (1965) 1328.
37. W. H. S. LAWSON and H. W. KERR, *Met. Trans.* **2** (1971) 2853.

Received 31 December 1975 and accepted 16 February 1976.